

# The Promise of GPS in Atmospheric Monitoring



Steven Businger,\* Steven R. Chiswell,\* Michael Bevis,\* Jingping Duan,\*  
Richard A. Anthes,+ Christian Rocken,# Randolph H. Ware,#  
Michael Exner,# T. VanHove,# and Fredrick S. Solheim#

## ABSTRACT

This paper provides an overview of applications of the Global Positioning System (GPS) for active measurement of the Earth's atmosphere. Microwave radio signals transmitted by GPS satellites are delayed (refracted) by the atmosphere as they propagate to Earth-based GPS receivers or GPS receivers carried on low Earth orbit satellites.

The delay in GPS signals reaching Earth-based receivers due to the presence of water vapor is nearly proportional to the quantity of water vapor integrated along the signal path. Measurement of atmospheric water vapor by Earth-based GPS receivers was demonstrated during the GPS/STORM field project to be comparable and in some respects superior to measurements by ground-based water vapor radiometers. Increased spatial and temporal resolution of the water vapor distribution provided by the GPS/STORM network proved useful in monitoring the moisture-flux convergence along a dryline and the decrease in integrated water vapor associated with the passage of a midtropospheric cold front, both of which triggered severe weather over the area during the course of the experiment.

Given the rapid growth in regional networks of continuously operating Earth-based GPS receivers currently being implemented, an opportunity exists to observe the distribution of water vapor with increased spatial and temporal coverage, which could prove valuable in a range of operational and research applications in the atmospheric sciences.

The first space-based GPS receiver designed for sensing the Earth's atmosphere was launched in April 1995. Phase measurements of GPS signals as they are occluded by the atmosphere provide refractivity profiles (see the companion article by Ware et al. on page 19 of this issue). Water vapor limits the accuracy of temperature recovery below the tropopause because of uncertainty in the water vapor distribution. The sensitivity of atmospheric refractivity to water vapor pressure, however, means that refractivity profiles can in principle yield information on the atmospheric humidity distribution given independent information on the temperature and pressure distribution from NWP models or independent observational data.

A discussion is provided of some of the research opportunities that exist to capitalize on the complementary nature of the methods of active atmospheric monitoring by GPS and other observation systems for use in weather and climate studies and in numerical weather prediction models.

## 1. Introduction

Soon after the launch of the space age, it was recognized that the predictable orbits of satellites provide

\*Department of Meteorology, University of Hawaii, Honolulu, Hawaii.

+University Corporation for Atmospheric Research, Boulder, Colorado.

#University Navstar Consortium (UNAVCO), Boulder, Colorado.  
*Corresponding author address:* Steven Businger, Dept. of Meteorology, University of Hawaii, 2525 Correa Road, Honolulu, HI 96822.

In final form 25 September 1995.

©1996 American Meteorological Society

a valuable reference frame for global navigation systems. Twenty years ago, the first Global Positioning System (GPS) tracking network was established by the U.S. military to link the satellite reference frame to Earth. The military network includes five globally distributed tracking stations that provide orbit determinations with 10-m accuracy. More recently, civilian organizations from various nations have established the International GPS Service network, which includes more than 50 globally distributed tracking stations and provides orbit determination with 50-cm accuracy in support of geodetic and geophysical research activities.

Today, the Global Positioning System consists of a constellation of 24 satellites that transmit L-band radio signals (~19- and 22-cm wavelengths) to large numbers of users engaged in navigation, time transfer, and relative positioning. A number of applications of meteorological utility have emerged as a product of this positioning technology. For example, as the cost and weight of GPS receivers have decreased, they are increasingly being used in balloon instrument transponders to provide location information and, thereby, information on layer-mean winds. There is also the possibility of using the receivers for quasi-Lagrangian air parcel tracking (e.g., Businger et al. 1996; Barat and Cot 1995). GPS technology can provide wind speed measurements with an accuracy of  $0.1 \text{ m s}^{-1}$ , is not susceptible to atmospheric electrical interference, and allows for simultaneous tracking of multiple balloons. These advantages, in addition to threats of the demise of the navigational aids loran (Long Range Navigation) and Omega, favor GPS systems for radiosonde and dropwindsonde applications (e.g., Boire et al. 1993). Accurate position and timing information is also crucial to research that uses the travel time of acoustic waves to probe global sea surface temperatures; the travel time of acoustic waves can then be related to the mean sea surface temperature along the path of the wave. This paper will focus on the application of GPS in active atmospheric measurement.

There are two primary methods by which GPS can be used to actively sense properties of the Earth's atmosphere. The first technique involves data collected by dual-frequency GPS receivers at fixed locations on the ground. GPS signals are delayed and refracted by the gases composing the atmosphere as they propagate from GPS satellites to the Earth-based receivers (Fig. 1). In particular, a significant and unique delay is introduced by water vapor because it is the only common atmospheric constituent that possesses a permanent dipole moment. This dipole moment is caused by an asymmetric distribution of charge in the water molecule, and it retards the propagation of electromagnetic radiation through the atmosphere. Per mole, the refractivity of water vapor is ~17 times that of dry air. Water's permanent dipole moment is also directly responsible for the unusually large latent energy associated with water's changes of phase, which in turn significantly impacts the vertical stability of the atmosphere, the structure and evolution of storm systems, and the meridional and radiational energy balance of the earth-atmosphere system. Thus, knowledge of the distribution of water vapor is essential in understand-

ing weather and global climate (Stephens and Greenwald 1991; IPCC 1992).

The sensitivity of atmospheric refractivity to the presence of water vapor makes it possible for Earth-based GPS receivers to provide time series data on integrated water vapor above the receiver site. The delay in propagation of microwave radiation to Earth-based receivers introduced by water vapor is referred to as the "wet delay" and is nearly proportional to the quantity of vapor integrated along the signal path. In liquid water and ice, the hydrogen bond between water molecules greatly reduces the contribution of the dipole moment to the delay. Thus, the presence of cloud water and ice does not discernibly affect the GPS measurement of water vapor. The ionospheric delay is dispersive (frequency dependent) and can be determined by observing both of the frequencies transmitted by GPS satellites and exploiting the known dispersion relations for the ionosphere (Spilker 1980; Brunner and Gu 1991). Ionospheric delays affecting observations recorded by a dual-frequency GPS receiver can be eliminated without reference to observations recorded by other GPS receivers in the same network. If the position of the receiver is accurately known and the ionospheric delay has been accounted for, an estimate of the vertically integrated water vapor overlying the receiver can be derived from the GPS signals and observations of surface temperature and pressure (Bevis et al. 1992, 1994; Rocken et al. 1993, 1995; Duan et al. 1996). Integrated water vapor represents the total latent heat available in the column from the vapor, and as such it has the potential to provide a powerful constraint to numerical weather prediction (NWP) models (Kuo et al. 1993, 1996) and in weather analysis.

A second approach for monitoring the Earth's atmosphere using GPS signals arises from efforts more than 30 years ago to study the atmospheres of other planets (see Melbourne et al. 1994 for a review). Coherent dual-band radio signals transmitted by a radio telescope to a spacecraft on the far side of a planet are bent through the planet's atmosphere on their way back to Earth, where a receiver picks up the signal. Profiles of the planetary atmosphere's pressure and temperature are then recovered from the two-way differential phase measurements (Melbourne 1976). Radio occultation, as this technique is called, has been used to probe the atmospheres and ionospheres of the planets and their moons, as well as certain physical properties of planetary surfaces and planetary rings (e.g., Fjeldbo et al. 1971; Lindal et al. 1981).

With the recent launch of a GPS receiver on a low Earth orbit (LEO) satellite (see the companion article by Ware et al. 1996), the radio occultation technique is now being applied to the Earth's atmosphere. When the GPS receiver aboard the LEO tracks a GPS satellite as it occults the Earth's atmosphere, the arrival time of the GPS signal at the receiver is delayed because of the refractive bending and slowing of the signal as it traverses the atmosphere (Fig. 1). By measuring the change in carrier phase over the entire occultation event (~60 s for the neutral atmosphere), the atmospheric refractive index can be determined as a function of altitude. Temperature and pressure profiles can then be derived through a downward integration using the known linear relationship between refractivity and density of dry air, the gas law, and the assumption of hydrostatic equilibrium.

Water vapor, the most variable and inhomogeneous of the major constituents of the troposphere, limits the accuracy of temperature recovery below the tropopause because of uncertainty in the water vapor distribution. However, the sensitivity of atmospheric refractivity to water vapor pressure means that refractivity profiles can in principle yield information on the global atmospheric humidity distribution and abundance, given independent information on the temperature and pressure distribution from NWP models or independent observational data (Gurvich and Krasil'nikova 1990; Gorbunov and Sokolovskiy 1993; Ware et al. 1996).

## 2. Earth-based GPS meteorology: A meteorological signal from geodetic noise

A primary task of geodetic GPS algorithms is to calibrate the delay or "equivalent excess path length" introduced by the refractivity of the Earth's atmo-

sphere. The ionosphere introduces a delay that can be determined and removed by recording the phase angles of the carriers of both of the frequencies transmitted by GPS satellites and exploiting known dispersion relations for the ionosphere (Spilker 1980). The remaining delay, due to the electrically neutral atmosphere, can be divided into two parts: a *hydrostatic*

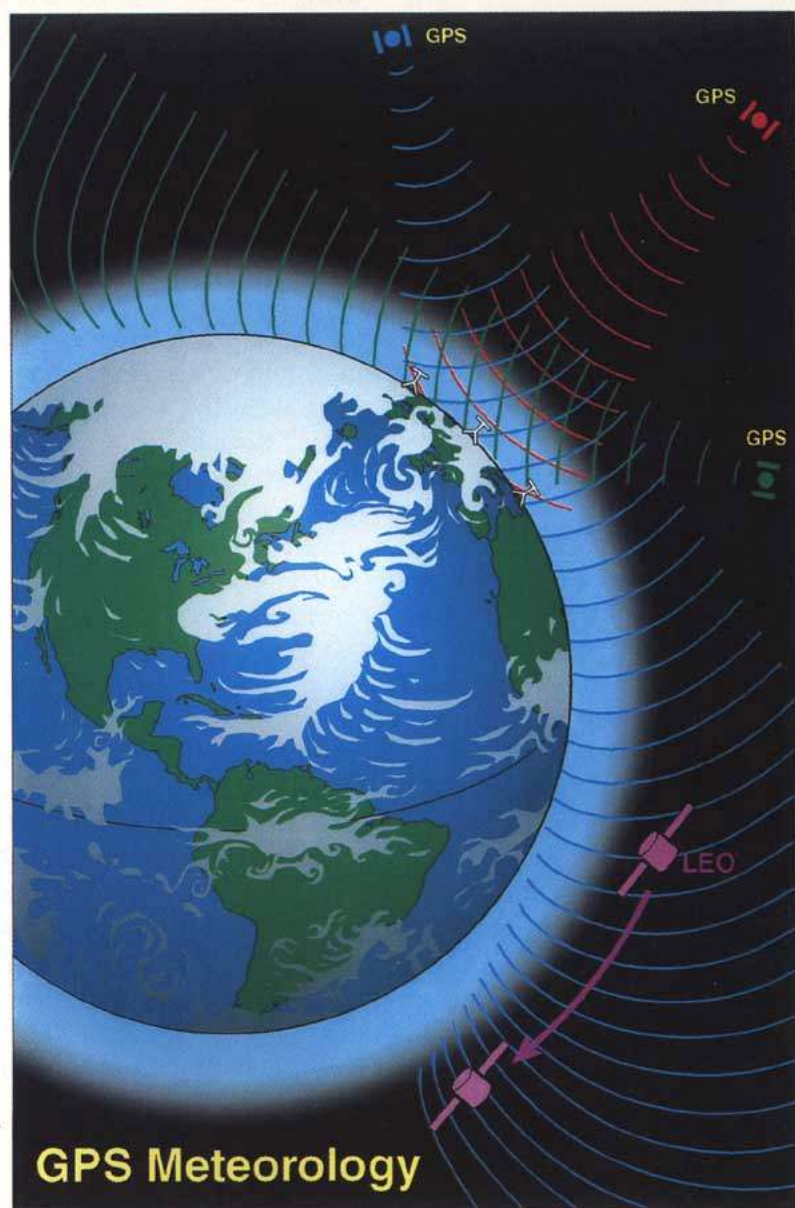


FIG. 1. A schematic diagram of GPS meteorology showing GPS signals passing from GPS satellites, orbiting at heights of ~20 000 km, through the intervening Earth's atmosphere to Earth-based receivers and to a low Earth orbit satellite. The delay of signals arriving at Earth-based receivers is proportional to the intervening integrated water vapor. Signals propagating from the GPS satellite to the LEO satellite at a height of about 775 km are refracted by the Earth's atmosphere during the ~60-s period before the signal is occulted by the Earth, providing a refractivity profile of the atmosphere.

delay and a wet delay (Saastamoinen 1972; Davis et al. 1985). Both delays are smallest for paths oriented along the zenith direction and increase approximately inversely with the sine of the elevation angle. Most expressions for the delay along a path of arbitrary elevation consist of the zenith delay multiplied by a mapping function that describes the dependence on elevation angle (Davis et al. 1985; Leick 1990). For example, assuming the atmosphere above a GPS antenna is azimuthally isotropic and neglecting the curvature of the Earth, the wet delay along a line with elevation angle  $e$  is related to the zenith wet delay by the mapping function  $(\sin e)^{-1}$ : wet delay equals zenith wet delay times  $(\sin e)^{-1}$ , where  $e$  is the elevation angle.

Since the hydrostatic delay is due to the transient or induced dipole moment of all the gaseous constituents of the atmosphere including water vapor, the term hydrostatic delay is favored over the sometimes used term "dry delay." The hydrostatic delay is well determined from pressure measurements, and at sea level it typically reaches about 2.3 m in the zenith direction. It is possible to calculate the zenith hydrostatic delay to better than 1 mm, given surface pressure measurements accurate to 0.3 mb or better. The basis for estimating the precipitable water in the atmosphere arises from the fact that the wet delay is closely related to the quantity of water vapor overlying the receiver. The zenith wet delay (ZWD) can be less than 10 mm in arid regions and as large as 400 mm in humid regions. Significantly, the daily variability of the wet delay usually exceeds that of the hydrostatic delay by more than an order of magnitude, especially in temperate areas (e.g., Elgered et al. 1990). Zenith wet delay can be estimated from GPS data as part of the overall least squares inversion for the coordinates of the GPS receivers, the orbital parameters of the GPS satellites, and other geodetic parameters of interest (Bevis et al. 1992; Rocken et al. 1993; Duan et al. 1996).

If we state integrated water vapor in terms of precipitable water (PW), the height of an equivalent column of liquid water is

$$PW = \int_0^{\infty} r \frac{\rho_a}{\rho_w} dz, \quad (1)$$

where  $r$  is the mixing ratio,  $\rho_a$  is the density of dry air, and  $\rho_w$  is the density of liquid water. It can then be shown (Askne and Nordius 1987; Bevis et al. 1994) that

$$PW = \Pi(ZWD), \quad (2)$$

where ZWD is given in units of length. The dimensionless constant of proportionality

$$\Pi = 10^6 \left[ \rho_w R_v \left( k_3 / T_m + k_2' \right) \right]^{-1} \quad (3)$$

is a function of empirical constants related to the refractivity of moist air ( $k_3$  and  $k_2'$ ), the gas constant for water vapor ( $R_v$ ), and a mean temperature of the atmosphere  $T_m$  defined (Davis et al. 1985) as

$$T_m = \frac{\int (e/T) dz}{\int (e/T^2) dz}, \quad (4)$$

where  $e$  is the water vapor pressure and  $T$  is the temperature.

As a rough rule of thumb, the ratio  $PW/ZWD = \Pi \sim 0.15$ , but the actual value of the parameter  $\Pi$  depends on the summation of the local climate controls (e.g., location, elevation, and season) and it can vary by as much as 15% (Bevis et al. 1992). Figure 2 shows the daily and seasonal variability in  $\Pi$  calculated from radiosonde data for Greensboro, North Carolina. It is significant that the amplitude of the daily fluctuations is of the same order of magnitude as that of the seasonal change. Nearly all of the spatial and temporal variability of  $\Pi$  is derived from the variability of  $T_m$ . Therefore, the accuracy with which a GPS-derived

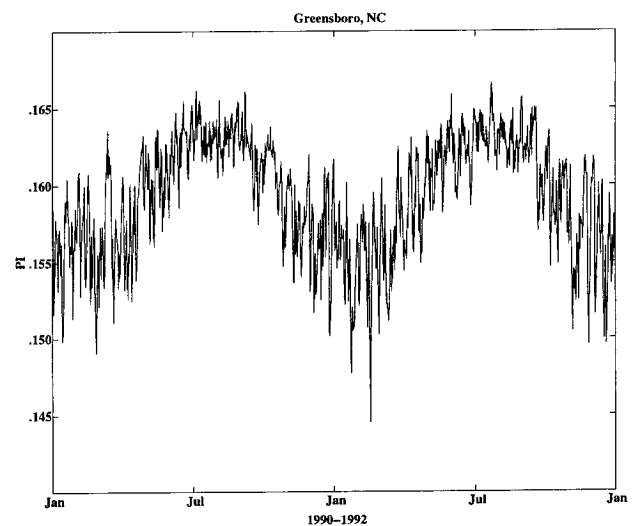


FIG. 2. Ratio of PW to ZWD, or  $\Pi$ , calculated for two years (January 1990 to January 1992) of radiosonde data from Greensboro, North Carolina.

ZWD estimate can be transformed into an estimate of PW is determined by the accuracy to which we can estimate the value of  $T_m$ . By using NWP models to estimate  $T_m$  at each GPS receiver as a function of time, one can estimate the coefficient  $\Pi$  used to map the ZWD onto PW with a relative error of less than  $\pm 1\%$  (Bevis et al. 1994). Alternatively, in an approach that is more convenient but slightly less accurate ( $\pm 2\%$ ), one can use a regression based on surface temperature and climatology (Bevis et al. 1992). Rocken et al. (1993) and Bevis et al. (1994) provide more comprehensive discussions of error sources.

Most GPS processing software packages in use today model the neutral atmospheric delay given the assumption of azimuthal isotropy. That is, mapping functions characterize line of sight (or *pointed*) delays solely in terms of the zenith delay and elevation angle measured from a *horizon*  $90^\circ$  from the local zenith. In fact, horizontal refractivity gradients, mainly associated with the inhomogeneity of water vapor, are known to produce azimuthal variations in delay (Ware et al. 1996). Algorithms have been developed to characterize azimuthal anisotropy (Herring 1992). To do so, it is necessary to increase the number of parameters from one (the zenith delay) to at least three and the number of predictor variables from one (elevation) to two (elevation and azimuth). The estimation of azimuthal variation is currently used in Very Long Baseline Interferometry analysis, and it is likely that this new class of mapping function will be incorporated in GPS processing on a routine basis. The advantages are twofold: taking proper account of azimuthal anisotropy will lead to better estimates of the zenith wet delay and, hence, PW, and information will be provided on the direction and magnitude of horizontal gradients in PW.

### 3. Results from the field

During May 1993, a field experiment called GPS/STORM was conducted to evaluate Earth-based

<sup>1</sup>The University Navstar Consortium (UNAVCO) provides equipment and assistance to academic investigators using GPS for scientific research. UNAVCO operates as a program of the University Corporation for Atmospheric Research and is supported by the National Science Foundation and NASA.

<sup>2</sup>GPS/STORM was funded by the National Science Foundation and was conducted in coordination with NOAA's Forecast Systems Laboratory Demonstration Division and the DOE Atmospheric Radiation Measurement program.

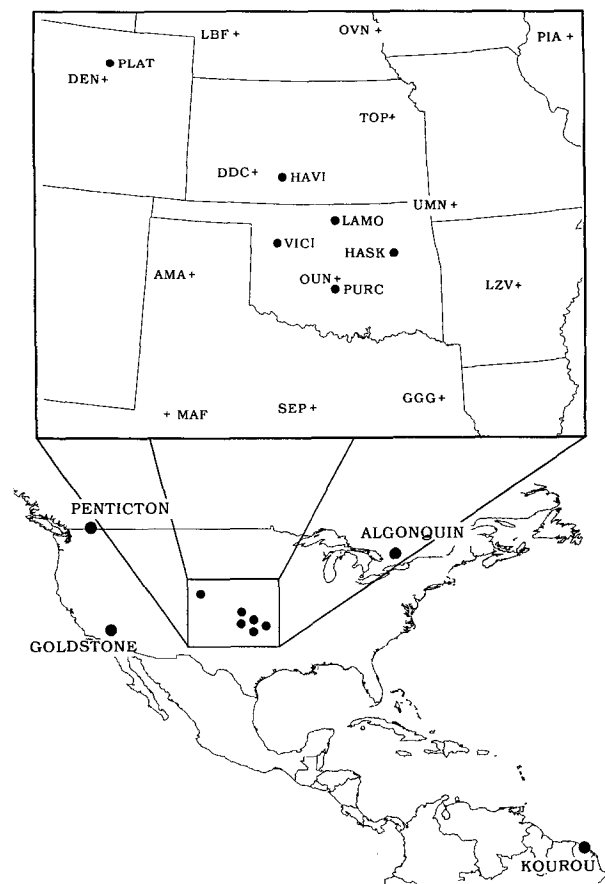


FIG. 3. (Top) Map of the GPS/STORM region showing the locations of the GPS receivers (●) and NWS radiosonde sites (+). (Bottom) Map showing remote GPS sites (labeled circles) used in absolute water vapor estimation.

GPS measurement of atmospheric water vapor in a region infamous for severe weather. During GPS/STORM, university and UNAVCO<sup>1</sup> scientists installed GPS receivers and ground-based microwave radiometers at five National Oceanic and Atmospheric Administration (NOAA) wind profiler sites and at the Department of Energy's (DOE) Southern Great Plains Cloud and Radiation Testbed sites near Lamont (LAMO), Oklahoma (Fig. 3, top).<sup>2</sup> The sites were chosen to take advantage of the existing operational infrastructure at the NOAA profiler sites. The mounted GPS receiver antenna is shown in Fig. 4.

To estimate the zenith wet delay (ZWD) and thus PW, knowledge of the station position and the satellite orbits is required. Precise orbits were obtained via the Internet from the International GPS Service (Zumberge et al. 1994) and from the Scripps Orbit and Permanent Array Center (SOPAC). During the field experiment, five or more satellites were typically



FIG. 4. Photograph of a GPS receiver antenna mounted on the perimeter fence of a NOAA wind profiler. The diameter of the antenna ground plane shown is ~50 cm.

visible at any time at each receiver site. For GPS networks with a separation between receivers of less than ~500 km, both the deterministic (least squares) and Kalman filtering techniques used to estimate zenith delay are more sensitive to relative rather than absolute delays (Rocken et al. 1993, 1995). This is because a GPS satellite observed by two or more receivers is viewed at almost identical elevation angles, causing the delay estimates to be highly correlated. Therefore, the estimates of ZWD derived from a small network are subject to an unknown bias for each sampling period. The value of the bias is constant across the whole network (i.e., the bias varies in time but not in space). One approach to estimating this bias is to measure PW with a ground-based water vapor radiometer (radiometer, hereafter) at a single reference site and use the GPS data to estimate PW relative to this reference site at any number of so-called secondary sites in the monitoring network. This procedure is known as *levering*. (One levers the group of biased PW estimates until they all have the correct absolute

value.) Rocken et al. (1995) show PW results using radiometer levering and find an rms error of ~1.5 mm and a bias of <0.5 mm when comparing PW from GPS receivers with that from radiometers.

An attractive alternate approach that eliminates the need for an independent measurement of PW at a reference site is to add a few outlying GPS stations to the receiver network that introduce baselines much longer than 500 km (e.g., Fig. 3). Provided GPS satellite orbit information of sufficient accuracy (~50 cm) is available, it is possible to estimate absolute ZWD and, therefore, absolute PW from the GPS observations alone. Rocken et al. (1995) noted that the difference, or error, between absolute PW estimation derived solely from GPS/STORM GPS data and that derived from radiometers was about 15% greater than the error when comparing radiometer-levered PW results with the radiometer PW values. Duan et al. (1996) included outlying GPS reference sites in Canada, California, and French Guiana (Fig. 3, bottom) and found errors slightly smaller than those obtained with radiometer levering. A complete description of the absolute estimation technique is given in Duan et al. (1996), which is the source of the GPS PW data in this paper. The radiometer data are from Rocken et al. (1995).

Subsequently, the NOAA's Environmental Research Laboratories, in an effort to implement the capability to monitor atmospheric water vapor in real time using GPS signal delay within NOAA, has coordinated a comprehensive comparison of GPS-derived PW data with radiometer PW data (NOAA 1995). The results of the tests show that when compared with rawinsonde observation, GPS-derived PW estimates are comparable in accuracy and precision to radiometer estimates. The reader is referred to the NOAA (1995) document for details of the statistics.

From a logistical perspective, the weather during GPS/STORM proved a major challenge. Hardware sustained considerable damage due to lightning strikes, including the loss of six personal computers used in data logging. However, GPS receivers escaped harm. During the period 6–9 May 1993, over 100 tornadoes, including an F-4 intensity tornado over Kansas, were reported in the general area of the field experiment, accompanying a slow-moving dryline. Previous research has documented the association of severe weather with such features (Schaefer 1974; McCarthy and Koch 1982; Parsons et al. 1991).

GPS-derived PW data from this period show fluctuations associated with the diurnal shift of the dryline

back and forth across the network (Fig. 5). Superimposed on the more gradual changes in PW associated with the changing position of the dryline are rapid changes in PW that appear in many cases to precede thunderstorm development (Fig. 5). These increases are consistent with moisture flux convergence, which has long been recognized as essential to convection (e.g., Kuo 1965). Charba (1979) found this quantity second only to the Modified Total-Totals index as a model output statistics predictor of local severe weather. Case studies (e.g., Waldstreicher 1989; Businger et al. 1991) have shown that storms often form in areas where moisture flux convergence is increasing rapidly with time and where the gradient in moisture flux convergence is tightening. Time series GPS PW data by themselves do not allow the forecaster to discriminate between advection and locate time-rate-of-change increases in PW at a single receiver site. However, in combination with other data sources, such as Doppler radar and satellites, the GPS PW time series have the potential to be valuable in short-term forecasting applications.

The scale of weather features that future GPS networks will be able to resolve spatially will depend in part upon the distance between receivers in the network. Figure 6 illustrates the impact of GPS PW data from five receiver sites on a synoptic objective analysis in the GPS/STORM region. Since moisture in this case was confined to the lower troposphere by a shallow capping inversion, the location of the dryline provides a qualitative reference for the accuracy of the analysis. The analysis using only radiosonde data shows relatively dry air over western Oklahoma (Fig. 6a), in conflict with the GPS data and in conflict with the analyzed position of the dryline shown in Fig. 6b. Qualitatively, the best agreement between the position of the dryline and the analysis of PW occurs in the heart of the GPS network, where the greatest concentration of supplemental data resides. The high PW value (32 mm) at Vici, Oklahoma, (VICI) is consistent with thunderstorm activity observed in that area and illustrates the degree of local variability in the distribution of atmospheric water vapor.

During the period 23–24 May 1993,

midtropospheric advection of relatively cold, dry air triggered convection and was associated with numerous reports of large hail and damaging winds in southern Oklahoma and northern Texas and several reports of funnel clouds or tornadoes in north Texas. Intrusions of cold, dry air at midlevels ahead of surface cold fronts or drylines have been described as cold fronts aloft (CFA) (Locatelli et al. 1989; Hobbs et al. 1990; Businger et al. 1991) and are not detected in standard surface observations. Figure 7 shows the drop in integrated water vapor at Purcell, Oklahoma, prior to the arrival of the surface front, illustrating the signature of this feature in the PW data. The advance of the cold front aloft across the surface cold front was a primary factor in the initiation of severe weather over the GPS/STORM region, because it generated convective instability and entrained dry air into thunderstorm downdrafts (Chiswell et al. 1996).

The temporal resolving power represented by the GPS data is demonstrated when a comparison is made between time series cross sections of equivalent potential temperature with and without the GPS PW data (Fig. 8). Combining radiosonde and GPS PW data can

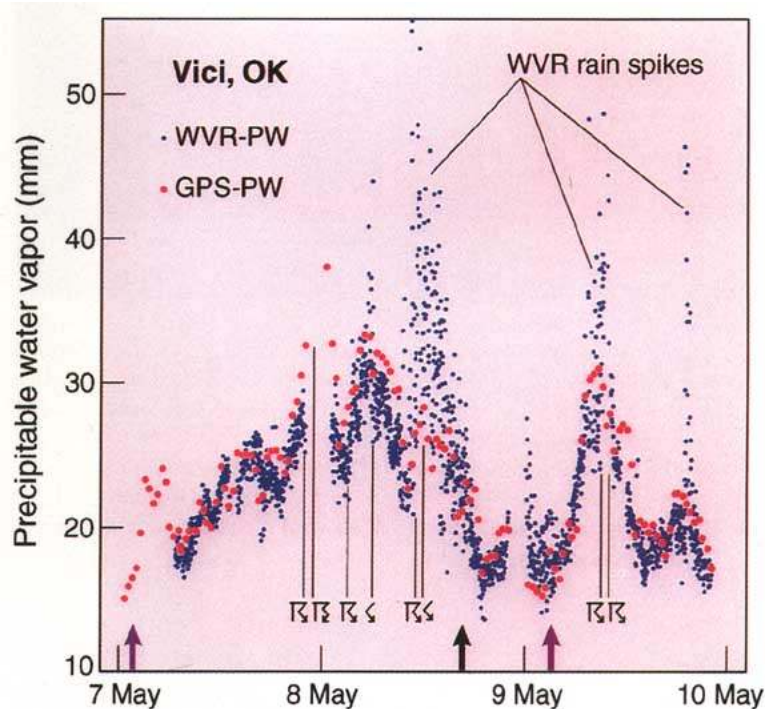


FIG. 5. Precipitable water at Vici for 1200 UTC 6 May to 0000 UTC 10 May 1994. The small blue dots represent radiometer measurements along the line of sight to GPS satellites, mapped to the zenith. The red dots represent 30-min averages of PW calculated from the least squares fits of GPS wet delay. Vertical arrows denote the time of the observed surface dryline passages at Vici. Time of thunderstorm activity is indicated with conventional symbols.

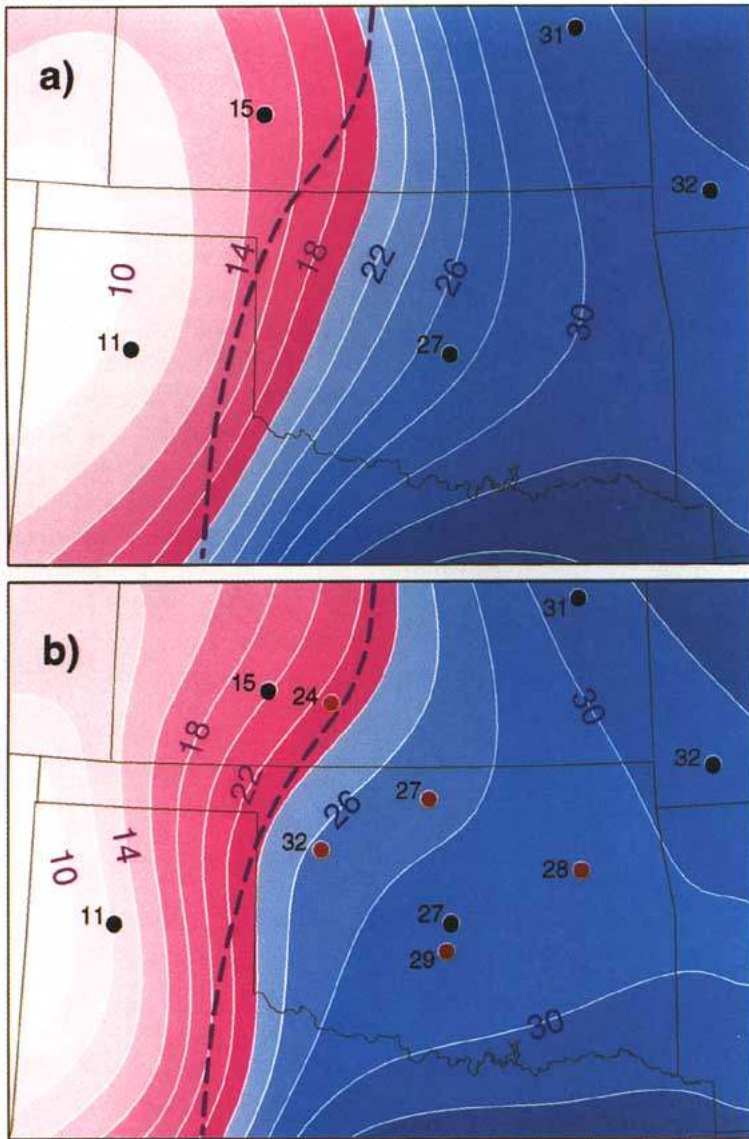


FIG. 6. (a) Objective analysis of precipitable water (in mm) using radiosonde derived PW data for 0000 UTC 8 May 1993. Small numbers indicate PW values at radiosonde sites (black circles). Purple dashed line in each panel indicates position of dryline analyzed by the National Meteorological Center. (b) Objective analysis of PW using radiosonde and GPS-derived PW data. Small numbers indicate PW values at radiosonde (black dots) and GPS sites (red dots) (adapted from Chiswell et al. 1996). The high PW value of 32 mm at Vici is consistent with thunderstorm activity observed in that area.

reveal more detail of the time evolution of the CFA than is available from NWP model output, satellite imagery, or radiosonde data alone. Water vapor density profiles can be obtained directly from radiosonde profiles (Fig. 8a) to obtain a time history of the evolution of the water vapor above a site.

The region of dry advection centered at ~600 mb can be distinguished from the more slowly changing

boundary-layer moisture (<850 mb) in the radiosonde data (Fig. 8a). Using the relationship between PW and vapor density ( $\rho_v$ )

$$PW = \rho_w^{-1} \int \rho_v dz, \quad (5)$$

where  $\rho_w$  is the density of liquid water, and also using radiosonde profiles of  $\rho_v$ , the GPS-measured PW can be used to constrain the analysis of  $\rho_v$  in the period between radiosonde releases. By requiring the integrated vapor density at each time in the analysis to agree with the value obtained from the GPS, while maintaining the boundary conditions imposed by the sounding data, the resulting analysis more accurately reflects the temporal evolution of the vapor density profile between sounding times (Fig. 8b). The result of this method shows the CFA base near 800 mb, with a considerably sharper gradient in vapor density than is available from sounding data alone or that which can be resolved over the relatively coarse grid of the National Meteorological Center's Nested Grid Model. The location of the enhanced gradient coincides in time with the onset of thunderstorms activity at Purcell and at Norman, Oklahoma.

The above case study examples from GPS/STORM are for illustrative purposes. Ongoing research will be required to more fully evaluate the utility of the Earth-based GPS PW data in weather analysis and forecasting as additional data from this method become available and are combined with other operational data sources and assimilated into NWP models. The reader is referred to Chiswell et al. (1996) for a more complete

description of the weather conditions surrounding the dryline, CFA cases reviewed here, and the application of GPS PW data in weather analysis.

In comparing the PW data from GPS and radiometers taken during GPS/STORM, an rms agreement of 1.0 to 1.5 mm is found (Duan et al. 1996). It is noteworthy that GPS measurements outperform those of the radiometers during periods of rain. Under these



conditions, the radiometer data are significantly degraded by the presence of water droplets on the microwave windows of the Radiometrics microwave radiometers deployed in the field experiment. The presence of rain, drizzle, or dew causes erroneously high and variable reports of PW, as seen in Figs. 5 and 7. This difficulty is a drawback in using the radiometer as a reference with which to lever a network of GPS receivers. By contrast, the absolute estimation technique, which relies only on GPS data, is not affected by precipitation.

#### 4. Discussion

The meteorological applications of GPS fall into two classes—those that require observations in near real time, such as numerical weather prediction, and those, such as climate studies, in which the delay between data collection and data processing is not an important issue. Climate studies make no demands related to timing but benefit from data that have been processed with the most precise orbits available (currently <0.5 m absolute error). The quality of the orbits improves as the number of tracking sites used to calculate the orbits increases. A benefit of the addition of a space-based receiver in the geometry of the Earth-based tracking network is the prospect of improved GPS orbits.

To be of greatest value to the operational forecasting community, data from Earth-based GPS networks and LEO receivers must be collected in a central location and processed with accurate GPS orbits, in near real time (within the hour).<sup>3</sup> High quality orbits (~0.5 m absolute error) are available from the International GPS Service 7 to 10 days after data collection. Since these orbits are used almost exclusively for postprocessing of survey and scientific data, this delay has not presented a problem. As the demand for real-time data for weather (and earthquake) prediction has risen, increased attention has been focused on the development of near-real-time orbits. Two possible approaches are

<sup>3</sup>For perspective, the processing time for GPS PW data can be compared with the time it takes (~2 h) for a radiosonde to ascend.

to compute GPS orbit corrections simultaneously with PW estimates or to make short-term (~1 day) orbit predictions. The Scripps Orbit and Permanent Array Center has recently initiated a rapid orbit determination using orbit predictions. SOPAC-predicted orbits have recently achieved an accuracy approaching that of the postprocessed orbits used in calculating the GPS/STORM PW data shown in this paper (Y. Bock 1995, personal communication).

A number of research opportunities exist for optimizing the complementary nature of the methods of active atmospheric monitoring by GPS described here and other observation systems currently in use. A few promising examples will be mentioned here. The space- and Earth-based approaches to monitoring the Earth's atmosphere are complementary in a number of ways.

- 1) Most Earth-based measurements involve vertical integration or averaging of atmospheric properties, whereas the space-based approach involves significant lateral averaging. Earth-based networks will be able to estimate lateral gradients in integrated water vapor at each station, whereas a single occultation event provides no significant information on lateral variability.

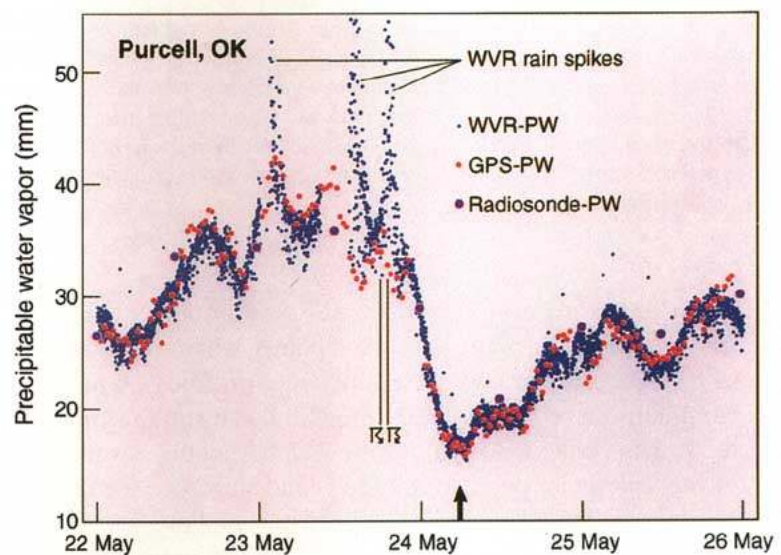


FIG. 7. Precipitable water at Purcell as measured by GPS, radiometer, and radiosonde from 0000 UTC 22 May to 0000 UTC 26 May 1993. The small blue dots represent radiometer measurements along the line-of-sight to GPS satellites, mapped to the zenith. The red dots represent 30-min averages of water PW calculated from the least squares fits of GPS wet delay. Twelve-hourly radiosonde data from Norman are shown by the purple dots. The vertical arrow denotes the time of the observed surface cold front passage at Purcell. Time of thunderstorm activity is indicated with conventional symbols.

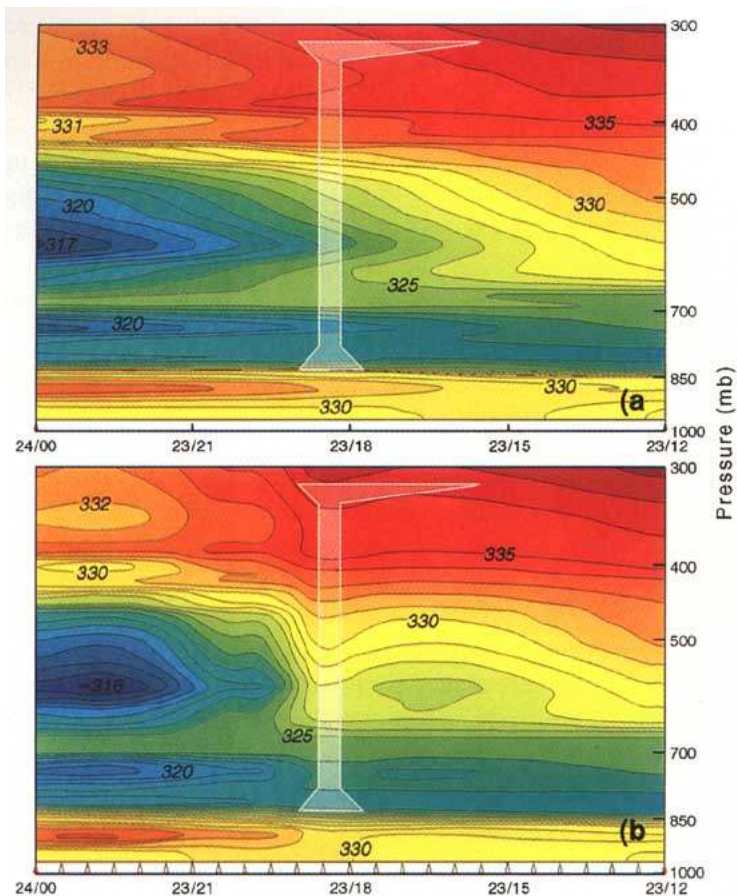


FIG. 8. (a) Time series cross section of equivalent potential temperature for 1200 UTC 23 May to 0000 UTC 24 May 1993 at Norman from radiosonde measurements. (b) Time series cross section of equivalent potential temperature with addition of GPS data constraints from Purcell. Cloud outline indicates time of thunderstorm activity. Small triangles along the bottom of the figure indicate times that GPS data are available. Labels along ordinate indicate date/UTC time (adapted from Chiswell et al. 1996).

- 2) Earth-based meteorology provides continuous measurements at a network of fixed points, whereas the space-based approach is discrete in time. Continuity in both space and time will be advantageous in contexts such as severe weather monitoring near major population centers and airports.
- 3) Because of the subhorizontal nature of its sampling geometry, space-based measurements are subject to obstruction by mountain ranges, and in adjacent low-lying areas, this may render much of the lower troposphere invisible.
- 4) Earth-based meteorology will never achieve good coverage over the oceans, whereas the space-based approach is essentially global. A GPS receiver in low Earth orbit with an inclination of at least  $65^\circ$

will provide refractivity profiles from approximately 500 GPS occultations per day distributed over the globe.

The relatively good vertical resolution and poor horizontal resolution of the GPS profiles are similarly complementary to those of nadir radiometric soundings. Preliminary results show that LEO-derived temperature soundings are comparable to radiosonde soundings in resolving the tropopause inversion (Ware et al. 1996). Knowledge of the spatial character of the tropopause has application in diagnosing potential vorticity anomalies and tropopause folds, which play a pivotal role in cyclogenesis (e.g., Hoskins et al. 1985). Over ocean areas, satellite radiometric radiances from operational polar and geostationary satellites are employed to construct soundings (Hayden 1988). Like soundings derived from Earth-based GPS receivers, radiometric soundings have high horizontal resolution and poor vertical resolution ( $\sim 3$  km). Since the measurement errors for these Earth- and space-based systems are largely independent, the estimation of atmospheric profiles of water vapor and temperature by a combined approach that includes data from Earth- and space-based GPS techniques and from satellite radiometer will be more accurate and provide better coverage than could be achieved by these methods alone (Suomi 1993).

The Earth- and space-based GPS techniques may be able to play a role in the development of a combined remote sensing capability that could eventually replace or reduce reliance on radiosondes. Integrated water vapor derived from Earth-based receivers can be distributed vertically according to ancillary information such as radiosonde or NWP model data (Chiswell et al. 1996). However, given a dense array of Earth-based receivers, the set of vectors from each receiver to each GPS satellite over a finite period of time represents a dense sampling of the troposphere above the array and could be processed using a technique similar to CAT scan tomography to provide information on the vertical distribution of water vapor. The vertical resolution provided by such an array

would depend upon the number of receiving antennas and their spatial distribution and is the subject of future research. There is potential for Earth-based GPS measurements to complement ground-based radio acoustic sounding system (RASS) measurements (Matuura et al. 1986), which provide information on the virtual temperature profile. The installation of GPS receivers at profiler sites in the Midwest, where RASS is also being tested, allows this potential to be investigated further (NOAA 1995). The opportunity for synergy between WSR-88D radar data and humidity data derived from GPS should also be mentioned.

The NWS is increasingly employing powerful workstations for data assimilation and graphical display to facilitate the analysis of new data streams from WSR-88D radars, the automated surface observing system, and satellites and to construct mesoscale forecasts for timely dissemination. In this context, GPS data can be incorporated in data assimilation systems for integration in mesoscale NWP models (Benjamin et al. 1991). Since the Earth-based GPS data represent the total integrated water vapor in the column, they provide a powerful constraint for NWP models. Mesoscale numerical model simulations have shown that when model-predicted precipitable water is relaxed toward an observed value, the model recovers the vertical structure of water vapor with an accuracy much greater than that found in statistical retrieval based on climatology, leading to improved short-range precipitation forecasts (Kuo et al. 1993). Data on the direction and magnitude of horizontal gradients in PW present an additional model constraint. Finally, data resolution over ocean areas in global NWP models should improve when refractivity profiles from space-based receivers are directly ingested. Studies with simulated space-based GPS profile data conclude that the optimum way of using the data in numerical weather prediction models may be to assimilate vertical profiles of atmospheric refractivity directly into the model (Eyre 1994; Zou et al. 1995), rather than separating temperature and humidity data first.

Concerns that arise in the context of GPS technology and real-time estimation are the effects of selective availability (SA) and antispoofing. The Department of Defense implemented SA in March 1990 in order to deny most civilian users of the system the maximum achievable accuracy in navigation applica-

tions by corrupting the signal structure. Although this policy has affected many civilian users of GPS, it has not had a significant impact on geodetic (relative positioning) applications (e.g., Rocken and Meertens 1991). Provided that all receivers sample the GPS signal close to simultaneously, the effect of SA can be eliminated after the fact. Consequently, SA is not a significant problem for GPS meteorology. However, it does affect the efficiency with which GPS processing applications can provide real-time estimates of PW for operational applications. Antispoofing is meant to stop false signals from misleading military receivers by encrypting the codes superimposed on both microwave carrier waves transmitted by the GPS satellite. New receiver architectures have addressed this issue.

The prospect of using Earth-based GPS data to measure atmospheric water vapor for research and operational weather forecasting is promising because extensive networks of continuously operating Earth-based GPS receivers are now being installed around the world by geophysicists, geodesists, surveyors, and others for a variety of scientific, engineering, and civilian navigation and positioning applications (Table 1, Fig. 9). GPS-derived PW data could be made available to the research and operational meteorological community at relatively little incremental cost.

Several hundred new private (communication) and government satellites have been announced for launching in the next several years (Ware 1992).<sup>4</sup>

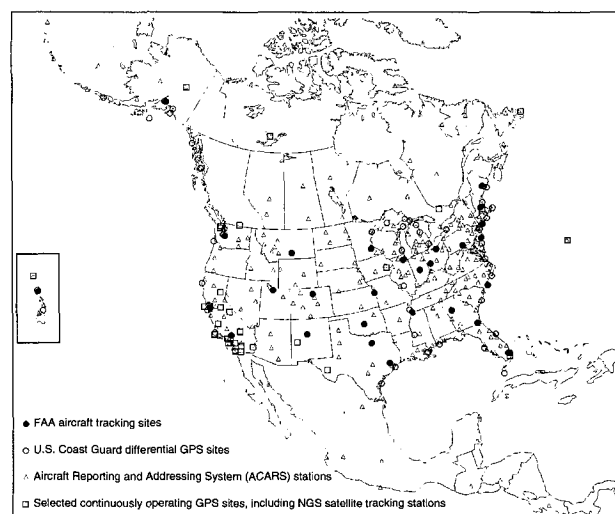


FIG. 9. Location of proposed Aircraft Reporting and Addressing System differential GPS Stations (triangles), proposed FAA aircraft tracking sites (●), selected continuously operating GPS sites including NGS satellite tracking stations (squares), and U.S. Coast Guard differential GPS sites (open circles).

<sup>4</sup>Satellites such as *TOPEX/POSEIDON*, *Gravity Probe-B*, *ARISTOTELES*, and *EOS-B* are carrying, or plan to carry, GPS receivers.

TABLE 1. Continuously operating Earth-based GPS receivers by network. Current GPS receivers are those already installed; proposed are those planned for installation in the near future (after Ware and Businger 1995).

Location	Current	Proposed	Sponsor
Antarctica	3	3	Australian and German governments/National Aeronautic and Space Administration (NASA)
Australia		7	Australian government
Canada	4	2	NASA
Canadian coastal stations		25	Canadian Coast Guard
Fennoscandia	16	8	Finnish, Norwegian, and Swedish governments
Japan		290	Japanese government
Mississippi Basin		15	U.S. Army Corps of Engineers
California	46	268	NASA/National Science Foundation (NSF)/U.S. Geological Survey (USGS)
Philippines		3	Australian and Japanese governments
U.S. airports	5	300	Federal Aviation Administration
U.S. coastal stations	6	50	U.S. Coast Guard
U.S. Midwest	4	28	NOAA
U.S. states	20	80	NGS/state governments
U.S. (other)		251	National Geodetic Survey (NGS)/NSF/USGS
Worldwide (other)	71	114	Defense Mapping Agency (DMA)/NASA/NSF/NGS/Other governments
<b>Subtotals</b>	<b>175</b>	<b>1444</b>	
<b>Total current and proposed</b>	<b>1619</b>		

Many of these satellites will carry GPS receivers for tracking and attitude measurements. With the demonstrated early promise of the GPS occultation technique for providing useful atmospheric data, the potential for gaining additional refractivity, temperature, and humidity data from this method is considerable. Due to

approaching that of radiosonde soundings. In principle, humidity profiles can be obtained from the refractivity profiles wherever the temperature distribution is known from other sources, such as radiosondes, or over tropical regions where horizontal and temporal variations in the temperature are small and

their global coverage, these data may provide the best opportunity to date for monitoring the global climate by observing changes in mean refractivity profiles (Yuan et al. 1993).

## 5. Conclusions

Measurement of atmospheric water vapor by Earth-based GPS receivers was demonstrated during the GPS/STORM field project to be comparable, and in some respects superior, to that by ground-based water vapor radiometers. Increased spatial and temporal resolution of the water vapor distribution from the GPS/STORM network proved valuable in monitoring the moisture flux convergence associated with thunderstorm development associated with an evolving dryline and the decrease in integrated water vapor associated with the passage of a midtropospheric cold front, both of which triggered severe weather over the area during the course of the experiment.

The first space-based GPS receiver designed for sensing the Earth's atmosphere was launched in April 1995. Preliminary results of this approach indicate that temperature profiles obtained from the refractivity data in the mid- to upper troposphere and lower stratosphere (Ware et al. 1996) can identify sharp temperature inversions characteristic of the tropopause with a resolution

reasonably well represented in global weather prediction models.

In conjunction with operationally available datasets, PW data from Earth-based receivers and refractivity profiles from space-based receivers represent a potentially important new resource for operational numerical weather prediction. The development of models that produce accurate orbit predictions is a step toward realizing this potential. Archived datasets from GPS networks and space-based receivers could prove valuable in basic research of mesoscale and synoptic-scale weather systems, the hydrologic cycle, and global climate change.

Although GPS measurements of the atmosphere have the potential to enhance the analysis and prediction of weather and climate, significant research is required to assess this potential in detail and to develop capabilities to derive maximum benefit from these new sources of atmospheric data. Further research is needed to determine how these data can most effectively be processed in combination with other data resources and assimilated into weather prediction models.

*Acknowledgments.* We would like to thank Seth Gutman (NOAA/FSL) and Ted Cress (Battelle NW) for their support of the GPS/STORM project. This research was supported by the National Science Foundation under Grants ATM-9207111, ATM-9496335, EAR-911756, and EAR-9116461. UNAVCO provided facilities and equipment under NSF Grant EAR-9116461. NCAR and NOAA/Environmental Testing Laboratory provided surface meteorological and additional radiometer data. Radiometrics Inc., Boulder, Colorado, loaned water vapor radiometers, and Paroscientific loaned a precise barometer for use in GPS/STORM.

## References

- Askne, J., and H. Nordius, 1987: Estimation of tropospheric delay for microwaves from surface weather data. *Radio Sci.*, **22**, 379–386.
- Barat, J., and C. Cot, 1995: Accuracy analysis of Rubsonde-GPS tracking wind sounding system. *J. Appl. Meteor.*, **34**, 1123–1132.
- Benjamin, S. G., and K. A. Brewster, R. Brummer, B. F. Jewett, T. W. Schlatter, T. L. Smith, and P. A. Stamus, 1991: An isentropic three hourly data assimilation system using ACARS aircraft observations. *Mon. Wea. Rev.*, **119**, 888–906.
- Bevis, M., S. Businger, T. A. Herring, C. Rocken, R. A. Anthes, and R. H. Ware, 1992: GPS Meteorology: Remote sensing of atmospheric water vapor using the Global Positioning System. *J. Geophys. Res.*, **97**, 15 787–15 801.
- , ———, ———, R. A. Anthes, C. Rocken, R. H. Ware, and S. R. Chiswell, 1994: GPS Meteorology: Mapping zenith wet delays onto precipitable water. *J. Appl. Meteor.*, **33**, 379–386.
- Boire, G., E. C. Souter, and S. P. Pryor, 1993: A low cost GPS rawinsonde system. Preprints, *Eighth Symp. on Meteorological Observations and Instrumentation*, Anaheim, CA, Amer. Meteor. Soc., 23–24.
- Brunner, F. K., and M. Gu, 1991: An improved model for the dual frequency ionospheric correction of GPS observations. *Manuscr. Geod.*, **16**, 205–214.
- Businger, S., W. H. Bauman III, and G. F. Watson, 1991: Coastal frontogenesis and associated severe weather on 13 March 1986. *Mon. Wea. Rev.*, **119**, 2224–2251.
- , S. R. Chiswell, W. C. Ulmer, and R. Johnson, 1996: Balloons as a Lagrangian measurement platform for atmospheric research. *J. Geophys. Res.*, in press.
- Charba, J. P., 1979: Two to six hour severe local storm probabilities: An operational forecasting system. *Mon. Wea. Rev.*, **107**, 268–282.
- Chiswell, S. R., S. Businger, M. Bevis, C. Rocken, R. Ware, T. VanHove, and F. Solheim, 1996: Application of GPS water vapor data in severe weather analysis. *Mon. Wea. Rev.*, submitted.
- Davis, J. L., T. A. Herring, I. I. Shapiro, A. E. Rogers, and G. Elgered, 1985: Geodesy by radio interferometry: Effects of atmospheric modeling errors on estimates of baseline length. *Radio Sci.*, **20**, 1593–1607.
- Duan, J., and Coauthors, 1996: GPS meteorology: Direct estimation of the absolute value of precipitable water. *J. Appl. Meteor.*, in press.
- Elgered, G., J. L. Davis, T. A. Herring, and I. I. Shapiro, 1990: Geodesy by radio interferometry: Water vapor radiometry for estimation of the wet delay. *J. Geophys. Res.*, **96**, 6541–6555.
- Eyre, J. R., 1994: Assimilation of radio occultation measurements into a numerical weather prediction system. ECMWF Tech. Memo. No. 199, 34 pp. [Available from ECMWF, Shinfield Park, Reading RG2 9AX, United Kingdom.]
- Fjeldbo, G. A., J. Kliore, and V. R. Eshleman, 1971: The neutral atmosphere of Venus as studied with the Mariner V radio occultation experiments. *Astron. J.*, **76**, 123–140.
- Gorbunov, M. E., and S. V. Sokolovskiy, 1993: Remote sensing of refractivity from space for global observations of atmospheric parameters. Max-Planck-Institut für Meteorologie Report No. 119. [ISSN 0937-1060.]
- Gurvich, A. S., and T. G. Krasil'nikova, 1990: Navigation satellites for radio sensing of the Earth's atmosphere. *Soviet J. Remote Sens.*, **7**(6), 1124–1131.
- Hayden, C. M., 1988: GOES-VAS simultaneous temperature-moisture retrieval algorithm. *J. Appl. Meteor.*, **27**, 705–733.
- Herring, T. A., 1992: Modeling atmospheric delays in the analysis of space geodetic data. *Proc. Symp. on Refraction of Transatmospheric Signals in Geodesy*, Delft, the Netherlands, Netherlands Geodetic Commission, 157–164.
- Hobbs, P. V., J. D. Locatelli, and J. E. Martin, 1990: Cold fronts aloft and the forecasting of precipitation and severe weather east of the Rocky Mountains. *Wea. Forecasting*, **5**, 613–626.
- Hoskins, B. J., M. E. McIntyre, and A. W. Robertson, 1985: On the use and significance of isentropic potential vorticity maps. *Quart. J. Roy. Meteor. Soc.*, **111**, 877–946.
- IPCC, 1992: *Climate Change 1992*. J. T. Houghton, B. A.

- Callander, and S. K. Varney, Eds., University of Cambridge Press, 200 pp.
- Kuo, H. L., 1965: On the formation and intensification of tropical cyclones through latent heat release by cumulus convection. *J. Atmos. Sci.*, **22**, 40–63.
- Kuo, Y.-H., Y.-R. Guo, and E. R. Westwater, 1993: Assimilation of precipitable water into a mesoscale numerical model. *Mon. Wea. Rev.*, **121**, 1215–1238.
- , X. Zou, and Y.-R. Guo, 1996: Variational assimilation of precipitable water using a nonhydrostatic mesoscale adjoint model, Part I: Moisture retrieval and sensitivity experiments. *Mon. Wea. Rev.*, in press.
- Leick, A., 1990: *GPS Satellite Surveying*. John Wiley & Sons, 352 pp.
- Lindal, G. F., and Coauthors, 1981: The atmosphere of Jupiter: An analysis of the voyager radio occultation measurements. *J. Geophys. Res.*, **86**, 8721–8727.
- Locatelli, J. D., J. M. Sienkiewicz, and P. V. Hobbs, 1989: Organization and structure of clouds and precipitation on the mid-Atlantic coast of the United States. Part 1: Synoptic evolution of a frontal system from the Rockies to the Atlantic coast. *J. Atmos. Sci.*, **46**, 1327–1348.
- Matuura, N., Y. Masua, H. Inuki, S. Kato, S. Fukao, T. Sato, and T. Tsuda, 1986: Radio acoustic measurement of temperature profiles in the troposphere and stratosphere. *Nature*, **323**, 426–428.
- McCarthy, J., and S. E. Koch, 1982: The evolution of an Oklahoma dryline. Part I: Meso- and subsynoptic-scale analysis. *J. Atmos. Sci.*, **39**, 225–236.
- Melbourne, W. G., 1976: Navigation between the planets. *Sci. Amer.*, **234**, 58–74.
- , and Coauthors, 1994: The application of spaceborne GPS to atmospheric limb sounding and global change monitoring. JPL Publication 94-18, 147 pp.
- NOAA, 1995: Precipitable water vapor comparisons using various GPS processing techniques. Document No. 1203-GP-36, 35 pp. [Available from NOAA ERL FSL, Boulder, CO.]
- Parsons, D. B., M. A. Shapiro, R. M. Hardesty, R. K. Zamora, and J. M. Intrieri, 1991: The finescale structure of a west Texas dryline. *Mon. Wea. Rev.*, **119**, 1242–1258.
- Rocken, C., and C. Meertens, 1991: Monitoring selective availability dither frequencies and their effect on GPS data. *Bull. Geodesique*, **65**, 162–169.
- , R. Ware, T. VanHove, F. Solheim, C. Alber, J. Johnson, M. Bevis, and S. Businger, 1993: Sensing atmospheric water vapor with the Global Positioning System. *Geophys. Res. Lett.*, **20**, 2631–2634.
- , T. VanHove, J. Johnson, F. Solheim, R. H. Ware, M. Bevis, S. Businger, and S. R. Chiswell, 1995: GPS/STORM—GPS sensing of atmospheric water vapor for meteorology. *J. Atmos. Oceanic Technol.*, **12**, 468–478.
- Saastamoinen, J., 1972: Atmospheric correction for the troposphere and stratosphere in radio ranging of satellites. *The Use of Artificial Satellites for Geodesy, Geophys. Monogr.*, Ser. 15, AGU, 247 pp.
- Schaefer, J. T., 1974: The life cycle of the dryline. *J. Appl. Meteor.*, **13**, 444–449.
- Spilker, J. J., 1980: Signal structure and performance characteristics. *Global Positioning System*, Vol. 1, The Institute of Navigation, 246.
- Stephens, G. L., and T. J. Greenwald, 1991: The Earth's radiation budget and its relation to atmospheric hydrology. 1. Observations of the clear sky greenhouse effect. *J. Geophys. Res.*, **96**, 15 311–15 324.
- Suomi, V. E., 1993: Final Report to Space System/Loral. [Available from Suomi Scientific, Inc., 10 Rosewood Circle, Madison, WI 53711.]
- Waldstreicher, J. S., 1989: A guide to utilizing moisture flux convergence as a predictor of convection. *Natl. Wea. Dig.*, **14**, 20–35.
- Ware, R., 1992: GPS sounding of Earth's atmosphere. *GPS World*, **3**, 56–57.
- , and S. Businger, 1995: Global positioning for geosciences research. *Eos, Trans. Amer. Geophys. Union*, **76**, 187.
- , C. Rocken, and K. Hurst, 1986: A GPS baseline determination including bias fixing and water vapor radiometer corrections. *J. Geophys. Res.*, **91**, 9183–9192.
- , and Coauthors, 1996: GPS sounding of the atmosphere from low Earth orbit: Preliminary results. *Bull. Amer. Meteor. Soc.*, **77**, 19–40.
- Yuan, L., R. Anthes, R. Ware, A. Rocken, W. Bonner, M. Bevis, and S. Businger, 1993: Sensing global climate change using the Global Positioning System. *J. Geophys. Res.*, **98**, 14 925–14 937.
- Zou, X., Y.-H. Kuo, and Y.-R. Guo, 1995: Assimilation of atmospheric radio refractivity using a nonhydrostatic mesoscale model. *Mon. Wea. Rev.*, **123**, 2229–2249.
- Zumberge, J., R. Neilan, and J. Kouba, 1994: The international GPS service for geodynamics—Benefits to users. Proc. Institute of Navigation, 7th Technical Meeting, Salt Lake City, UT, 1663–1666.

